

***Development, Characterization
and Applications of a Non
Proprietary Ultra High
Performance Concrete for
Highway Bridges***

**Sherif El-Tawil, Mouhamed Alkaysi,
Antoine E. Naaman, Will Hansen
and Zhichao Liu**

***Department of Civil and Environmental Engineering
University of Michigan, Ann Arbor, Michigan***

Intentionally left blank

1. Report No. RC-1637	2. Government Accession No. N/A	3. MDOT Project Manager Steve Kahl	
4. Title and Subtitle Development, Characterization and Applications of a Non Proprietary Ultra High Performance Concrete for Highway Bridges		5. Report Date 03/14/2016	
		6. Performing Organization Code N/A	
7. Author(s) Sherif El-Tawil, Mouhamed Alkaysi, Antoine E. Naaman, Will Hansen and Zhichao Liu		8. Performing Org. Report No. N/A	
9. Performing Organization Name and Address University of Michigan Room 1038 Wolverine Tower 3003 South State Street Ann Arbor, MI 48109		10. Work Unit No. (TRAIS) N/A	
		11. Contract No. 2013-0068	
		11(a). Authorization No. Z1	
12. Sponsoring Agency Name and Address Michigan Department of Transportation Research Administration 8885 Ricks Rd. P.O. Box 30049 Lansing MI 48909		13. Type of Report & Period Covered Final Report 3/30/2013 – 3/14/2016	
		14. Sponsoring Agency Code N/A	
15. Supplementary Notes N/A			
16. Abstract Ultra-high performance concrete (UHPC) is a new class of cementitious materials that have exceptional mechanical and durability characteristics. UHPC is commercially available. However, its cost for construction of highway structures is prohibitive. Based on an extensive testing program, a new family of non-proprietary UHPC materials with excellent characteristics in compression and tension, as well as exceptional resistance to freeze-thaw and chloride ion penetration were developed. The most cost effective of these deviates from traditional UHPC mixtures in that it uses a 50:50 mix of Portland Type I and Ground Granulated Blast-Furnace Slag (GGBS) as a binder, lacks any silica powder (inert filler) and requires no post-placement treatment. The use of GGBS improves the material's 'greenness' making it a more sustainable cementitious product. Specifications for making the new UHPC were proposed. The developed UHPC blend was then used to conduct a comprehensive study on bond between UHPC and deformed steel bars to facilitate and enable future structural applications. Bond pull out tests showed the developed UHPC requires significantly reduced development lengths in order to attain steel bar yield compared to traditional concrete. Models to characterize the bond strength were proposed and a UHPC joint consisting of two pre-cast bridge deck elements was developed and tested at full scale. It was shown that a 6" (150 mm) joint made of the developed UHPC was sufficient to successfully transfer loading between the decks.			
17. Key Words Ultra-high performance concrete, non-proprietary, durability, strength, bond, joints, precast concrete, bridge, freeze-thaw		18. Distribution Statement No restrictions. This document is available to the public through the Michigan Department of Transportation.	
19. Security Classification - report Unclassified	20. Security Classification - page Unclassified	21. No. of Pages	22. Price N/A

Intentionally left blank

DISCLAIMER

This publication is disseminated in the interest of information exchange. The Michigan Department of Transportation (hereinafter referred to as MDOT) expressly disclaims any liability, of any kind, or for any reason, that might otherwise arise out of any use of this publication or the information or data provided in the publication. MDOT further disclaims any responsibility for typographical errors or accuracy of the information provided or contained within this information. MDOT makes no warranties or representations whatsoever regarding the quality, content, completeness, suitability, adequacy, sequence, accuracy or timeliness of the information and data provided, or that the contents represent standards, specifications, or regulations.

Intentionally left blank

ACKNOWLEDGEMENT

This project was funded by the Michigan Department of Transportation. The authors would like to acknowledge the support and efforts of Mr. Steve Kahl and Mr. David Juntunen for initiating and directing this research. The authors also wish to acknowledge the continuing assistance of the Research Advisory Panel (RAP) members in contributing to the advancement of this study. The authors acknowledge the help and ideas of Prof. Kay Wille of the University of Connecticut, Storrs, who served as a consultant on this project. Parts of this work were conducted by the second author in fulfillment of his PhD dissertation requirements at the University of Michigan.

Intentionally left blank

Table of Contents

List of Figures	5
List of Tables	9
EXECUTIVE SUMMARY	1
1. INTRODUCTION	5
1.1. Ultra-High Performance Concrete (UHPC).....	5
1.2. Research Objectives.....	5
1.3. Organization of the Report.....	7
2. BACKGROUND AND LITERATURE REVIEW	9
2.1. Strength of UHPCs.....	9
2.1.1. Compressive and Tensile Behavior of UHPC	9
2.1.2. Effect of Silica Fume	10
2.1.3. Effect of Silica Powder	11
2.1.4. Cements Effects on UHPCs	11
2.1.5. Effect of Fiber Type and Quantity	12
2.2. DURABILITY OF UHPCs	12
2.2.1. Freeze-Thaw Resistance	12
2.2.2. Chloride Ion Penetration Resistance:.....	13
2.3. Bond Development in UHPCs	14
2.3.1. Bond Development of Steel Bars Embedded in UHPC.....	14
2.3.2. Lap Splice & Component Tests with UHPC	15
3. MATERIAL PERFORMANCE AND CHARACTERIZATION	17
3.1. OVERVIEW.....	17
3.2. EXPERIMENTAL PARAMETERS AND PROCEDURE	18
3.2.1. UHPC Material Properties and Cost.....	18
3.2.2. Steel Fibers.....	21
3.2.3. Mixing Procedure.....	22
3.2.4. Tensile Strength Testing:	23
3.2.5. Compression Testing:	25
3.3. RESULTS AND DISCUSSION	26
3.3.1. Analysis of Data.....	26
3.3.2. Overview of Results.....	27

3.3.3.	Cement Type.....	29
3.3.4 -	Silica Powder.....	30
3.3.4.	Silica Fume	33
3.3.5.	Fiber Content	35
3.3.6.	Cost Analysis	39
3.4.	CONCLUSION	40
4.	DURABILITY PERFORMANCE OF UHPC.....	43
4.1.	OVERVIEW.....	43
4.2.	EXPERIMENTAL PARAMETERS.....	43
4.2.1.	UHPC Mix Designs	43
4.2.2.	Experimental Procedure.....	45
4.2.3.	Air Void Analysis	47
4.2.4.	Rapid Chloride Penetration Test.....	48
4.2.5.	Compressive Strength Testing	49
4.3.	EXPERIMENTAL RESULTS.....	49
4.3.1.	Freeze-Thaw Resistance	49
4.3.2.	Air Void Analysis	53
4.3.3.	Rapid Chloride Permeability.....	56
4.4.	DISCUSSION OF EXPERIMENTAL RESULTS	59
4.5.	CONCLUSION	62
5.	FACTORS AFFECTING BAR BOND DEVELOPMENT FOR UHPC.....	65
5.1.	OVERVIEW.....	65
5.2.	EXPERIMENTAL PARAMETERS AND PROCEDURE:	65
5.2.1.	Bar Pull Out Testing Program and Test Set Up.....	65
5.2.2.	Lap Splice Joint Testing Program.....	69
5.2.3.	Material Properties.....	71
5.2.4.	Bar Pull Out Results	72
5.2.5.	Effect of Embedment Length.....	74
5.2.6.	Effect UHPC Cast Orientation on Bond	81
5.2.7.	Effects of Fiber Volume Content.....	83
5.2.8.	Early Age Testing of UHPC on Bond.....	84
5.2.9.	Bar Pull Out vs. Lap Splice Beam Results	86

5.2.10.	Design Implications	88
5.3.	CONCLUSION	89
6.	SIMPLIFIED UHPC JOINTS FOR BRIDGE CONSTRUCTION	93
6.1.	OVERVIEW.....	93
6.2.	DESIGN OF THE EXPERIMENTAL PROGRAM.....	93
6.2.1.	Pure Flexure vs. Combined Shear and Flexure Testing.....	94
6.2.2.	Joint Details & Selection	95
6.2.3.	Specimen Design	96
6.2.4.	Specimens Tested and Material Parameters	98
6.3.	EXPERIMENTAL PROCEDURE	100
6.3.1.	Test Set Up.....	100
6.3.2.	Instrumentation	100
6.4.	MATERIALS	101
6.5.	CONSTRUCTION OF THE PRECAST CONCRETE SPECIMENS	102
6.6.	RESULTS AND DISCUSSION	104
6.6.1.	Comparison of Calculated Bar Stress versus Measured Bar Stress.....	104
6.6.2.	F-100 Specimen Tests.....	105
6.6.3.	F-150 and F-200 Specimens	106
6.6.4.	Effect of Fiber Content in Pure Flexure.....	108
6.6.5.	Effect of Joint Size.....	109
6.6.6.	Combined Shear and Flexure Testing.....	110
6.6.7.	Effect of Fiber Content in Combined Shear and Flexure	111
6.7.	FINITE ELEMENT MODEL AND PARAMETRIC STUDY.....	112
6.7.1.	Model Setup	112
6.7.2.	UHPC and Concrete Material Models	113
6.7.3.	Parametric Study.....	115
6.7.4.	Model Validation	116
6.7.5.	Results of Parametric Study.....	116
6.8.	CONCLUSION	119
7.	SUMMARY, MAJOR CONCLUSIONS AND FUTURE RESEARCH	121
7.1.	SUMMARY AND MAJOR CONCLUSIONS.....	121
7.2.	PROMISE AND COMMERCIAL POTENTIAL OF UHPC	122

7.3.	AN OPPORTUNITY FOR THE STATE OF MICHIGAN.....	123
7.4.	A BRIGHT FUTURE	123
7.5.	FUTURE RESEARCH NEEDS	124
8.	REFERENCES	125
9.	APPENDIX A – STRESS-STRAIN PLOTS FOR ALL UHPC MIXES	135
9.1.	WHITE CEMENT MIXES	136
9.2.	PORTLAND TYPE V CEMENT MIXES.....	139
9.3.	GGBS/PORTLAND TYPE I CEMENT MIXES	142
10.	APPENDIX B – RESULTS OF FREEZE-THAW TESTING – RILEM.....	143
11.	APPENDIX C – DETAILS FROM BAR PULL-OUT TESTING.....	145
12.	APPENDIX D – DETAILS OF BEAM TESTING.....	177
13.	APPENDIX E – SPECIAL PROVISIONS	195

List of Figures

Figure 2-1 Typical Tensile Strain Response in UHPC	10
Figure 3-1 Grain Size Analysis for Sand	19
Figure 3-2: Example of the Steel Fibers Used in this Study	22
Figure 3-3 Mixing process (photos courtesy of Prof. Kay Wille)	23
Figure 3-4 Tensile test set up, (b) Instrumentation, (c) Specimen dimensions.....	24
Figure 3-5: Tensile and Compression Specimens Post Test.....	26
Figure 3-6: Effects of Different Cements on UHPC for Mixes with 1.5% Volume Fiber Content	31
Figure 3-7: Effects of Silica Powder Contents on UHPC for Mixes with 1.5% Volume Fiber Content.....	32
Figure 3-8: Effect of Silica Fume Contents on UHPC for Mixes with 1.5% Volume Fiber Content.....	34
Figure 3-9: Effects of Lower Steel Fiber Volume Contents on UHPC	36
Figure 3-10: Strain Response for UHPC Specimens in Tension	38
Figure 3-11: Strain (%) Capacity as function of Steel Fiber Content.....	39
Figure 3-12: Compressive Strength as a function of Cost Index	40
Figure 4-1: Freeze Thaw Test Close-Up (17).....	46
Figure 4-2: Specimen with Test Surface Facing the Bottom under Frozen Condition.....	46
Figure 4-3: Temperature Profile of Freeze-Thaw Test.....	47
Figure 4-4: Treated and Untreated UHPC Cross Section for Air Void Analysis	48
Figure 4-5: Mass Loss of UHPC Mixes after at Least 60 Cycles.....	51
Figure 4-6: a. Effect of Silica Powder on Mass Loss; b. Average Mass Loss as a Function of Silica Powder Quantity	52
Figure 4-7: Average Mass Loss as a Function of Cement Type.....	52
Figure 4-8: Air Content by LTM and PCM	54
Figure 4-9: Air Content as a Function of Power's Spacing Factor.....	55
Figure 4-10: a. Air Content as a Function of Silica Powder Percent, b. Average Air Content as a function of Silica Powder.....	56
Figure 4-11: Average Air Content as a Function of Cement Type.....	56
Figure 4-12: Total Charge Passed for UHP C and RC Mix.....	57
Figure 4-13: a. Total Coulombs passed as a function of Silica Powder Percent; b. Average Coulombs passed as a function of Silica Powder	58
Figure 4-14: Average Coulombs passed as a function of Cement Type.....	59

Figure 4-15: Particle Size Distributions for UHPC Mixes and Regular Concrete	61
Figure 4-16: Moisture Uptake and RDM% for UHPCs (27).....	62
Figure 5-1: (a) Test Set Up for Bar Pull Out (b) and Instrumentation and Load Path for Specimen	66
Figure 5-2: (a) Fibers Aligned Parallel to Bar (b) Fibers Aligned Transversely to Bar	68
Figure 5-3: Construction and Reinforcement Details for Precast Decks with UHPC Joint	70
Figure 5-4: Four Point Bending Test Set Up for Flexure Test for Specimens F-100-1P-1, F-100-1P-2, F-100-2P-1 and F-100-2P-2	71
Figure 5-5: (a) Bar Fracture, (b) Bar Slip, and (c) Conical Concrete Failure.....	72
Figure 5-6: Force Slip for 13 mm bars at (a) 100 mm, (b) 75 mm, and (c) 50 mm embedment, (d) Peak Bond Stress vs. Embedment Length	76
Figure 5-7: Idealized Reaction of Reinforcing Steel Embedded in Concrete, Subjected to Tension, Cross Sectional View	77
Figure 5-8: Force Slip for 16 mm bars at (a) 100 mm, (b) 75 mm, and (c) 50 mm embedment, (d) Peak Bond Stress vs. Embedment Length	78
Figure 5-9: Force Slip for 19 mm bars at (a) 100 mm, (b) 75 mm, and (c) 50 mm embedment, (d) Peak Bond Stress vs. Embedment Length	80
Figure 5-10: (a) Comparison of Bond Data for 16 mm Epoxy Coated Bar and (b) scatter of the current data available for 13 mm, 16 mm, and 19 mm bars	82
Figure 5-11: (a) Force Slip for 16mm bars with Parallel and Transverse Fibers, (b) Force Slip for 19 mm bars with Parallel and Transverse Fibers, and (c) Bond Stress Comparison (Dark Gray- 19 mm bars, Light Gray – 16 mm bars).....	83
Figure 5-12: (a) Force Slip for 16 mm bars with 1% and 2% Fibers, (b) Force Slip for 19 mm bars with 1% and 2% Fibers, and (c) Bond Stress Comparison (Dark Gray – 19 mm bars, Light Gray – 16 mm bars)	85
Figure 5-13: (a) Force-Slip Curve, (b) Bond Stress – Relative Slip, (c) Compressive Strength and (d) Bond Stress Data for Early Age Tests.....	86
Figure 5-14: Average Bond Stresses in lap splices vs. bar pull out specimens.....	88
Figure 5-15: Maximum Average Bar Stress under Direct Pull Out.....	89
Figure 6-1: Shear and Moment forces in beams under (a) pure flexure loading and (b) combined shear and flexure testing	95
Figure 6-2: Joint Dimensions and Reinforcement Details	97
Figure 6-3 Joint Shape Details for the 150 mm (a), 200 mm (b) joint, Lap Splice Connection Detail (c)	99
Figure 6-4: Instrumentation of the Precast Bridge Deck Beams	101
Figure 6-5: Deformed 16 mm Epoxy Reinforcement Bar	102

Figure 6-6: Forms and Placed Bars (a), Lap Splice (b), Poured UHPC Joint (c), and Set up with DIC (d)	103
Figure 6-7: Comparison of Calculated and Measured Bar Stresses	105
Figure 6-8: (a) DIC of 100 mm joint specimens, (b) Splitting Failure in deformed specimen, (c) Load-Deflection Curves for 100 mm specimens with 2% fibers and (d) 100 mm specimens with 1% fibers	106
Figure 6-9: (a) DIC of 150 mm joint specimens, (b) Splitting Failure in deformed specimen, (c) Load-Deflection Curves for 150 mm specimens and (d) 200 mm specimens.....	108
Figure 6-10: Maximum Force in F-100 Decks at a Function of Fiber Volume Content	109
Figure 6-11: Moment at Joint as a function of Joint Width.....	110
Figure 6-12: (a) DIC of 100 mm joint, SF specimens, (b) Splitting Failure in deformed specimen, (c) Load-Deflection Curves for 100 mm specimens, 1% fiber by vol. and (d) 100 mm specimens, 2% fiber by vol.....	112
Figure 6-13: (a) Finite Element Model and (b) Mesh for F-150-2P Specimens.....	113
Figure 6-14: Typical UHPC Tensile Response for Joint Fill Material	114
Figure 6-15: (a) Original Joint Design for FEA, (b) non-tapered joint design, and (c) flat joint design.....	115
Figure 6-16: Experimental FEA Load-Deflection for (a) 150 mm joints and (b) 200 mm joints	118
Figure 6-17: (a) Un-deformed shape, (b) deformed shape and (c) von Mises Strain for 150 mm, (d) Plot of the cracks developed and (e) and Damaged Beam after Testing, Actual joint.....	118

Intentionally left blank

List of Tables

Table 3-1: Chemical and Physical Properties of Materials.....	19
Table 3-2: Mixture Proportions by Weight with Cost Index	20
Table 3-3: Cement Properties	21
Table 3-4: Cost and Performance Summary.....	28
Table 3-5: UHPC Mix Design and Ratios	40
Table 4-1: Mixes Proportions for UHPCs tested	44
Table 4-2: Summary of Test Results	50
Table 4-3: Chloride Permeability Rating.....	57
Table 5-1: Experimental Parameters and Number of Tests	69
Table 5-2: Test Results for Simple Bar Pull Out	73
Table 5-3: Test Results Beam Lap Splice Tests	87
Table 6-1: Main Variable of Beam Specimens.....	99
Table 6-2: Summary of Results from Experimental Testing.....	104
Table 6-3: Material Parameters for FEM.....	114
Table 6-4: Summary of Simulated Beams	116

Intentionally left blank

EXECUTIVE SUMMARY

Introduction:

Ultra-high performance concrete (UHPC) is a cementitious material that achieves a compressive strength of at least 22 ksi (150 MPa) and has self-consolidation properties. It is comprised of component materials with particle sizes and distributions carefully selected to maximize packing density. The high packing density, which means that constituent particles are arranged as compactly as possible, is the reason for the extremely high mechanical and durability properties of the material.

UHPC is commercially available at the present time. However, its cost for construction of highway structures is prohibitive. A non-proprietary version of UHPC was recently developed at the University of Michigan (UM). While significantly cheaper than the cost of commercial products, the cost of the UM version is still relatively high and can be substantially reduced through optimization of its constituent components while still maintaining the extraordinary properties that make UHPC such an exceptional building material.

Objectives:

The primary objective of this project is to develop a cost-optimized version of non-proprietary UHPC and characterize its mechanical and durability properties. Another key objective is to investigate the possibility of using UHPC for field-cast joints that commonly occur in precast construction. Specific objectives include:

- Identify a low cost, non-proprietary UHPC mix design through cost-optimization of the constituent components while still maintaining the exceptional properties of UHPC.

- Characterize the strength and durability properties of the optimized mixture, focusing specifically on tensile and compressive strengths, freeze-thaw resistance and rapid chloride penetration resistance.
- Quantify the bond between UHPC and deformed steel bar reinforcement for a range of parameters and loading scenarios associated with feasible bridge applications.
- Investigate the use of UHPC bridge field joints between precast regular concrete decks.

Summary of Research:

Some of the component materials of UHPC are substantially more expensive than those used in regular concrete. To optimize cost, research was conducted to investigate the relationship between material performance and the type or amount of the most expensive components, i.e. cement, silica fume and silica powder. Short-term material performance was assessed via tensile and compressive tests and durability properties were evaluated based on freeze-thaw and chloride ion penetration testing as well as quantification of the presence and distribution of air voids. The test results were used to optimize cost versus performance characteristics of the UHPC blends considered. At the structural level, a comprehensive study investigating the bonding between UHPC and deformed bars was carried to investigate the effect on bond of bar size, type, embedded length, fiber content, fiber orientation and curing age. Using this data, new joints making use of UHPCs superior bond characteristics were constructed and tested in order to prove a quick and simple method for the assembly of precast bridge elements.

Summary of Results:

From the material testing program, a low cost UHPC material with excellent characteristics in compression and tension, as well as exceptional resistance to freeze-thaw and chloride ion

penetration was developed. The proposed mix deviates from traditional UHPC mixtures in that it uses a 50:50 mix of Portland Type I and Ground Granulated Blast Furnace Slag (GGBS) as a binder, lacks any Silica Powder (inert filler) and requires no post-placing treatment. The cost of the cementitious material ingredients was reduced by half compared to available non-proprietary UHPCs available at the onset of this research. The use of GGBS improves the material's 'greenness' making it a more sustainable cementitious product. Specifications for making the new UHPC were proposed.

The developed UHPC blend was then used to conduct a comprehensive study on bond between UHPC and deformed steel bars to facilitate and enable future structural applications. Bond pull out tests showed the developed UHPC requires significantly reduced development lengths in order to attain steel bar yield compared to traditional concrete. Models to characterize the bond strength were proposed and a UHPC joint consisting of two pre-cast bridge deck elements was developed and tested. It was shown that a 150 mm (6 inch) joint was sufficient to successfully transfer loading between the decks.

The Promise of UHPC - An Opportunity for the State of Michigan:

UHPC derives its unique properties from its high packing density and the presence of steel fibers. The special constituents of UHPC make it more expensive than regular concrete. However, they also give it its exceptional short- and long-term properties. In particular, the extremely high freeze-thaw resistance, negligible chloride penetration, and ability to mobilize the material's strain hardening response in tension to limit crack width, suggests that UHPC structures can be extremely long-living and low maintenance at the same time. Such structures will have inherently low life cycle costs, in spite of relatively higher initial costs.

UHPC is currently in its infancy and this project is an important early step. Additional research on fiber optimization, mixing technology and structural testing is needed to fully realize the material's promise. These research topics represent an opportunity for the State of Michigan to take leadership in steel fiber production, a key component of UHPC. The State, with its focus on vehicle manufacturing, is well suited to be major fiber industry hub given that steel fibers are made from chopped high strength wires that are used in steel-belted tire products.

1. INTRODUCTION

1.1. Ultra-High Performance Concrete (UHPC)

Ultra-high performance concrete is a new class of cementitious materials that achieve a compressive strength of at least 22 ksi (150 MPa) (Wille et al. 2014, Graybeal 2014, Wille et al. 2012, Wille et al. 2011). When properly reinforced with steel fibers, UHPCs can achieve strain hardening behavior and display compressive and direct tensile strengths as high as 35 ksi (242 MPa) and 2 ksi (14 MPa), respectively (Graybeal, 2003). Changes in the type and quantity of steel fibers directly affect the ductility, durability and strength of the material (Wille et al. 2011; Kim et al. 2011, 2010a, 2010b, 2010c, 2008a, 2008b, 2008c, 2008d, 2007). UHPC also exhibits exceptional energy absorption prior to crack localization (Pyo et al. 2015a, 2015b, 2013a, 2013b, 2013c) and self-consolidation properties (Graybeal, 2006).

Recent developments in UHPC at the University of Michigan have led to new, non-proprietary formulations that are cheaper than the patented versions (Wille et al, 2011). The new formulation described in Wille et al. (2011) is made up of components readily available on the US open market, does not require any special mixing or placing equipment and has a higher ductility than other commercially available products (Rigaud et al., 2012). Relative to traditional concretes, the price of the non-proprietary UHPC in Wille et al. (2011) remains high, but still it is substantially less than its patented commercial equivalent.

1.2. Research Objectives

With strengths in compression approaching that of mild steel, finding new uses for UHPCs is intriguing many practitioners, who want to use the material in their projects. However, broad

usage is hindered by the high cost of the material and lack of test results, and understanding in general, of UHPCs behavior at the structural level. With these issues in mind, the objectives of this research project are:

- Survey and identify potential applications for non-proprietary UHPC particularly for Accelerated Bridge Construction (ABC) and Precast Bridge Element Systems (PBES).
- Investigate whether a family of new UHPC materials can be made using locally available components and optimize the cost by tailoring of the mix, while still maintaining ultrahigh performance characteristics.
- Characterize the properties of the new family of UHPCs, focusing on tensile strength, compressive strength, modulus of elasticity, and durability by laboratory testing.
- Conduct pullout tests of steel reinforcing bars from UHPC to investigate the bond strength between steel bars with various coatings and the surrounding UHPC matrix.
- Investigate using computational and experimental methods to simulate the behavior of UHPC field joints (closure pours).
- Develop detailed guidance (special provisions) for making the proposed UPHC on a construction site.
- Assess the life cycle performance of UHPC in light of the experimental results.
- Propose future research efforts using the developed UHPC.

1.3. Organization of the Report

The main body of the report is preceded by detailed contents including lists of figures and tables. This is followed by an introduction giving briefly the scope and objectives of the study and importance of the topic.

- Chapter 2 outlines the previous works involving UHPC that are of interest to the topics covered in this report.
- Chapter 3 covers an investigation into how material properties change as a result of variations in the amount and/or type of individual components. The chapter aims to optimize the cost of UHPC with respect to its strength.
- Chapter 4 investigates the durability of select UHPC mixes identified in chapter 3 through freeze-thaw testing, rapid chloride penetration testing and air void characterization.
- Chapter 5 gives an in depth study into the factors affecting bond between UHPC and reinforcing steel.
- Chapter 6 studies the use of UHPC in precast bridge constructions via experimental testing and finite element analysis.
- Chapter 7 provides a summary of the research, the most important conclusions and future work.

All chapters are preceded by a brief synopsis of the chapter. References which have been used for certain inputs are listed at the very end of the report.

Intentionally left blank

2. BACKGROUND AND LITERATURE REVIEW

2.1. Strength of UHPCs

2.1.1. Compressive and Tensile Behavior of UHPC

The high compressive strength of UHPC is well known and established (Graybeal, 2014). Larrard and Sedran (1994) produced a concrete mortar with a compressive strength of 35 ksi (236 MPa). Wille, Naaman and El-Tawil (2011) were able to prepare UHPCs with 28-day compressive strengths in excess of 30 ksi (200 MPa) without requiring the use of expensive post treatment techniques. Graybeal (2006) has shown that UHPC reaches a peak stress of around 22 ksi at 0.003 strains (0.3%). Wille and Naaman (2011) showed that when reinforced with steel fibers, UHPC mixes were able to achieve 0.6% strain capacity in tension prior to strain softening. More information regarding the tensile and compressive behavior of UHPCs can be found in the works by Wille (2011) and Graybeal (2003, 2006, and 2014).

UHPC not only has a higher tensile strength than conventional concrete, it can also exhibit strain hardening response after initial cracking when properly reinforced with steel fibers. The typical stress strain curve for ultra-high performance concrete is shown in Figure 2-1. Following the definitions set forth by Naaman (Naaman & Reinhardt, 2007), the first part of the material's tensile behavior is elastic, which continues up until the specimen develops an initial crack at what is known as the first cracking strength point (σ_{cc} , ϵ_{cc}) in Figure 2-1. Following this, the material then exhibits strain hardening up until its peak point (σ_{pc} , ϵ_{pc}). The strain hardening behavior of segment II is typically characterized by multiple crack development in the gauge length of the specimen. Following the strain-hardening region, the material then begins to exhibit crack localization (segment III). This segment of the curve is best represented by a stress versus

crack opening response but many researchers continue to describe the region as a stress versus strain relationship, based on the nominal gage length of the specimen, as is done herein.

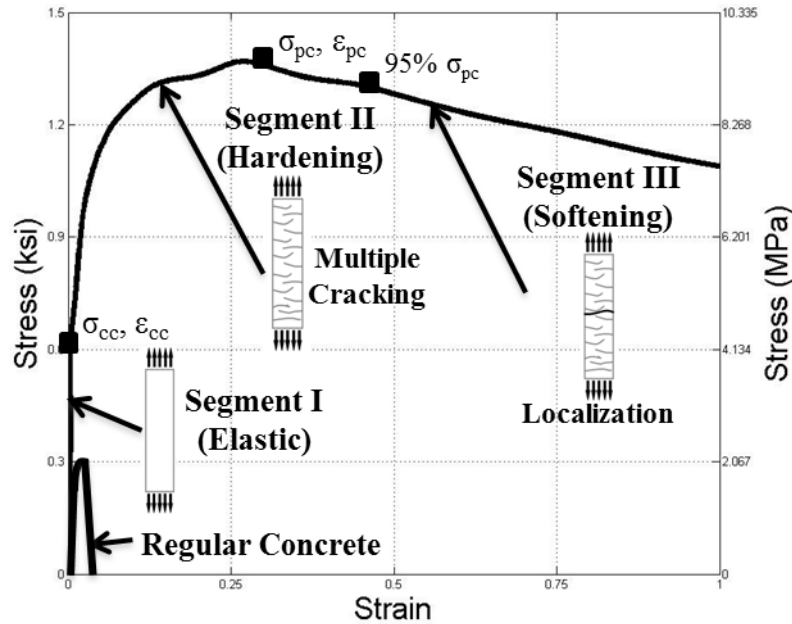


Figure 2-1 Typical Tensile Strain Response in UHPC

2.1.2. Effect of Silica Fume

Most UHPCs contain silica fume and silica powder. Silica fume is a reactive powder with pozzolonic properties. Silica powder is an inert powder, used primarily to increase the density of the cementitious matrix. Several research studies have investigated the effects of silica fume (SF) on the behavior of UHPCs. Rong, Xiao and Wang (2014) investigated the effects of SF on the hydration and microstructure of UHPCs, concluding that SF dominated the hydration process at lower water-binder ratios. Rong et al. (2015) also partially replaced cement with SF in UHPCs and determined the flexural and compressive strengths were highest when the content of SF was approximately 3% to binder, and decreased at higher contents due to the agglomeration of SF particles. Brouwers et al. (2014) similarly investigated the effect of SF on the UHPC hydration

process and material behavior, concluding that an optimal ratio of 3.74% SF to binder yields the highest mechanical properties of UHPC. Oertel et al. (2013) reported that the nearer the dispersion of silica particle sizes match to those in the primary mixture particle sizes, the further the compressive strengths increase in UHPCs. Wille (2015) studied the effects of various SFs on the compressive behavior in UHPCs, and reported compressive strengths ranging from 20 ksi to 26 ksi. To the authors' knowledge, no work has been done on the effect of silica fume on the direct tensile properties of UHPCs.

2.1.3. Effect of Silica Powder

To date, little work has been done to investigate the effects of Silica Powder (SP) on the tensile and compressive performance of UHPCs. Wille (2011) researched the effects of SP on UHPCs ranging from 0 SP-binder to 0.5 SP-binder ratios, finding a ratio of 0.3 SP to cement yielded the highest compressive strength. As with silica fume, to the knowledge of the authors, no work has been done evaluating the effect of different silica powder quantities in UHPCs under direct tension.

2.1.4. Effect of Cement

Additionally, little work has been done to investigate the effects of various cements on the material behavior of UHPC. Yu and Brouwers (2015) used fly ash (FA), ground granulated blast-furnace slag (GGBS) and limestone powder (LP) to replace cement in UHPC mixes, determining UHPCs with the GGBS has higher mechanical properties at 28 and 91 days than with other cements they considered. Wille (2015) investigated the compressive strengths for UHPCs substituting several different cements, yielding strengths between 19 ksi (130 MPa) and 32 ksi

(221 MPa). To date, no work quantifies the effects of cement type on the tensile response of UHPCs.

2.1.5. Effect of Fiber Type and Quantity

Several papers currently discuss the effects of fiber content, shape, size and topology on ultra-high performance concretes. The addition of steel fibers into the ultra-high performance concrete matrix leads to enhanced material performance such as a high tensile capacity, ductility, reduced crack spacing, and high energy dissipation capability. The magnitude of these effects is a direct result of the fiber material strength, cementitious matrix – fiber bond ability, fiber aspect ratio (length: diameter), fiber volume content and fiber surface topology. Pyo (2015) investigated the strain rate dependent tensile properties of UHPCs with different fibers and fiber volume contents. Wille (2011) investigated the tensile performance of UHPCs with fiber contents as low as 1%. Yu and Brouwers (2015) investigated hybrid fiber UHPCs containing a combination of hooked, short and long straight fibers, at 2% volume contents. They concluded that the combination of several fiber types yields ultra-high performance while using fewer fibers. To date, no work has been done investigating the effect of low fiber contents (<1%) on the compressive and tensile performance of UHPC.

2.2. DURABILITY OF UHPCs

2.2.1. Freeze-Thaw Resistance

Tests investigating UHPCs resistance to freeze-thaw have been limited. Ahlborn et al. performed freeze-thaw cycling tests in accordance to ASTM C 666 (2008), procedure B, showing that after 32 freeze-thaw cycles, ultra-high performance concrete specimens showed no degradation. Acker and Behloul (2004) similarly reported that after 300 freeze-thaw cycles, UHPC showed no

degradation. Pierard et al. (2012) reported that specimens achieving strength between 20.3 ksi (140 MPa) and 23.2 ksi (160 MPa) also showed no degradation after 112 cycles. Graybeal (2006) performed air void analyses on Ductal[®], finding UHPC void numbers to be between 0.2 and 7.5 voids/in (0.008 and 0.30 voids/mm), corresponding to an air content of 5.7% to 7.3% with no vibration.

To date, no research has been done to investigate the durability parameters for a non-proprietary blend of UHPC. Further, no testing has been done to investigate the effects of various material parameters on the durability of UHPC. Yazici (2008) looked into the effect of silica fume and high-volume Class C fly ash on the durability of self-compacting concretes, determining that a 10% by volume inclusion of silica fume resulted in enhanced freeze-thaw resistance, accompanied by increased compressive strengths. Work by Alexander and Magee (1999) evaluated the durability of concretes containing condensed silica fumes and ground granulated blast furnace slag (GGBS), determining blends containing these materials outperformed regular concretes in durability testing of water absorption.

2.2.2. Chloride Ion Penetration Resistance:

Performing rapid chloride permeability tests, Ahlborn (2008) showed that UHPC was capable of achieving permeability values less than 100 coulombs for both air-cured and steam-cured specimens. Materials with coulomb values less than 100 are generally considered to have negligible chloride ion penetration. Testing two different types of reactive powder concretes, Bonneau (1997) showed that specimens were able to achieve 6 to 9 coulombs. Graybeal (2006) reported that untreated specimens achieved coulomb values of 360 and 76 at 28 days and 56 days respectively. Most of the existing chloride permeability studies pertain to proprietary materials and data for non-proprietary blends is lacking at present.

2.3. Bond Development in UHPCs

2.3.1. Bond Development of Steel Bars Embedded in UHPC

There is limited published data on the bonding behavior between UHPCs and steel reinforcement bars. Graybeal (2010, 2014) performed pull out tests for #4, #5, and #6 bars embedded 3, 4 and 5 inches (75, 100 and 125 mm) respectively into UHPC cylinders, with all of the steel bars fracturing before bond failure. Graybeal (2014) recently has shown that under static conditions, UHPC specimens are capable of developing a bond stresses of approximately 2.9 - 5 ksi (20 – 35 MPa) in bar pull out specimens and are largely dependent on bar spacing, concrete cover, and development length and bar size. In a different study, Swenty and Graybeal (2012) performed pull out tests on #4 bars embedded into 6 in (150 mm) concrete cubes. Two different UHPC mixes were used, one achieving bar fracture and the other achieving bar yield. Performing pull out tests on 12 mm diameter bars, varying concrete cover and embedment lengths, Fehling et al. (2012) determined that increasing cover widths and embedment lengths increased the bond stress, reaching those sufficient for bar yield. Holschemacher et al. (2004) reported achieving bond stresses up to 8.7 ksi (60 MPa) using 12 mm bars in UHPC cylinders. Saleem et al. (2013) investigated the development length requirements for high strength steel bars in UHPC, concluding that 10 mm and 22 mm (#3 and #7 U.S. sizes) bars require $12 d_b$ and $18 d_b$ to develop adequately. Jungworth et al. (2004) performed tests on 20 mm and 12 mm diameter bars, reaching bond stresses of 5.5 ksi (38 MPa) and 9.5 ksi (66 MPa). Of the literature currently available on bond, data only exists on testing performed using Ductal® or Ceracem®, both proprietary concretes. No published data currently exists for non-proprietary UHPCs. As discussed later on, there is much discrepancy in existing data regarding the maximum achieved

bond stress during the pull out tests, with some studies reporting values as high as 9.5 ksi (66 MPa), or as a low as 1.4 ksi (9.8 MPa) (Graybeal, 2010).

2.3.2. Lap Splice & Component Tests with UHPC

Component level testing with UHPC remains largely confined to highway infrastructure projects. The Federal Highway Administration has released several reports on test installations on existing structures. UHPC was used in concrete waffle slab decks in an accelerated bridge construction in Wapello County, Iowa showing that UHPC is a viable material for infrastructure redesign (Wipf et al, 2011). New York D.O.T. also tested a live installation of a UHPC joint using hooked bars and a small joint width, also concluding exceptional joint performance for the UHPC (FHWA, 2014).

Steinberg et. al. (2010) investigated the structural reliability of pre-stressed UHPC flexure models for bridge girders showing that acceptable levels of reliability can be obtained using typical AASHTO procedures. Graybeal (2014) released a series of tests evaluating the joint force transfer capacity of UHPC under various parameters, including type of bars, size of bars etc. He concluded that UHPC was able to act as a closure pour joint between two precast decks more efficiently than traditional grouts and concretes at splice lengths as little as 6 inches (150 mm). Of these tests performed so far, all of them have made use of Ductal.

Few studies have investigated the splice length requirements for UHPC joints. Graybeal recently investigated the splice length of pre-stressing strands in field cast UHPC connections, concluding that 12 mm and 15 mm diameter strands require 20 inches (510 mm) and 24 inches (610 mm) to fully develop (Graybeal, 2015). Hoonhee and Park (2014) investigated the lower limits of contact splice lengths in precast, steam-cured UHPC beams under flexure, determining a lap

splice length greater than 6 in. (150 mm) was required to cause yield in the bars. Both of these studies were performed using Ductal, i.e. no studies currently exist for non-proprietary UHPCs, as provided herein. Furthermore, to the author's knowledge no studies exist investigating the UHPC's performance in non-contact lap splices between two precast beam elements, as done herein.

3. MATERIAL PERFORMANCE AND CHARACTERIZATION

3.1. OVERVIEW

This chapter investigates the performance of several new UHPC mix designs with a focus on minimizing cost. Performance parameters include compressive strength and full tensile stress-strain characterization. The experimental variables are four different quantities of silica fume, three different quantities of silica powder, three different cement types (white cement Type I, Portland cement Type V, GGBS/Portland cement Type I blend) and three different fiber volume contents (0.5%, 1.0%, and 1.5%) of straight, smooth, high strength steel fibers. Experimental results showed minor differences in mechanical behavior due to variations in the quantity of silica fume. Silica powder changes led to little difference in material behavior, suggesting that silica powder can be removed due to its high cost. UHPCs containing white cement Type I exhibited the best performance in almost all aspects of behavior including load carrying capacity, energy absorption capacity and multiple cracking behaviors, but carried the highest cost. Specimens containing the GGBS/Portland cement Type I binder showed lower performance, but at decreased cost. UHPC specimens containing 0.5% fibers exhibited some strain hardening behavior, which became more pronounced as the fiber volume fraction increased. The results suggest that fiber volume contents of 1.0% or 1.5% could significantly reduce the chance for crack localization under dead load or working conditions, respectively, in structural applications.

3.2. EXPERIMENTAL PARAMETERS AND PROCEDURE

3.2.1. UHPC Material Properties and Cost

UHPC, depending on the types and quantity of reinforcing fibers added to the cementitious mixture, carries a high cost. Currently, commercially available proprietary blends cost \$2,000/yd³ (\$2615/m³) and includes 2% steel fibers by volume (Ahlborn, 2008). This is 15 - 20 times higher than the cost of conventional concrete. Using current prices, the UHPC recently developed at the University of Michigan (Wille, 2011) carries a lower cost of materials (\$516/yd³ without fibers, \$1,029/yd³ with 2% fibers).

The cement used in the initial development of the UHPC in Wille et al. (2011) was a Portland Type I white cement. This cement has a high C₃S content (74%), and a moderate fineness (3930 cm²/g Blaine Value) as well as a low C₃A content (less than 5%). The particle sizes and costs for each UHPC constituent is listed in Figure 3-1 shows the grain size distributions for the two types of sands, F12 and F100 used in this research. The materials are obtained from reputable suppliers and the costs specified are valid for 2013 when the bulk of the research was conducted.

In Wille et al. (2011), the optimal cement to silica fume to silica powder ratio was determined to be 1 C: 0.25 SF: 0.25 SP, with a w/c ratio of 0.22 and a compressive strength of 27.8 ksi (192 MPa). Maintaining the w/c ratio established in the previous work, Table 3-2 lists the mix proportions and associated costs (without fibers) for all of the mixes considered in this work. Cost is listed as a cost index in order to simplify the discussion later on. The cost index is simply the ratio of the mix's cost compared to the starting mixture published in Wille (2011), based on current prices in the US. The index is a relative indicator of cost, since actual costs will vary in time and by location. The first entry, W-25-25, represents the original mix ratio in (Wille, 2011).

	Median	10% of Particles	90% of Particles	
Cement	10 – 20 μm	3 μm	40 μm	
Silica Fume	0.1 – 1 μm	0.1 μm	10 μm	
Silica Powder	10 – 20 μm	1 μm	40 μm	
F12 Sand	500 μm	Larger than 300 μm	Smaller than 1000 μm	
F100 Sand	100 μm	Larger than 50 μm	Smaller than 300 μm	
	Silica Fume		Silica Powder	
SiO ₂	Minimum 85%	SiO ₂	Maximum 90%	
H ₂ O	Maximum 3%	H ₂ O	Maximum 1%	
Pozzolonic Activity	Minimum 105%	Pozzolonic Activity	N/A	

Table 3-1: Chemical and Physical Properties of Materials

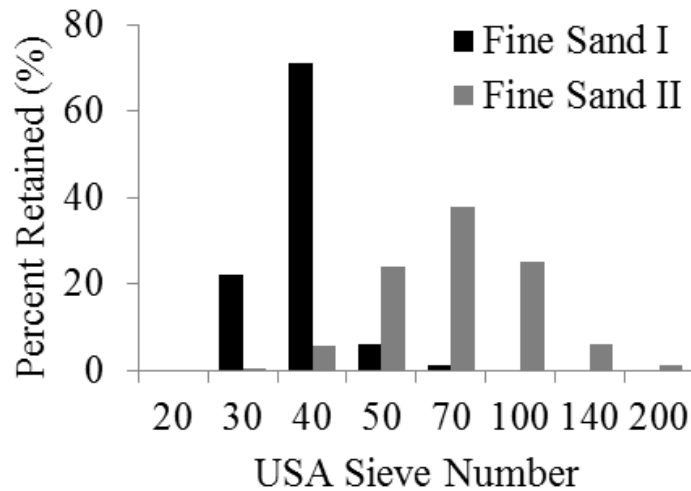


Figure 3-1 Grain Size Analysis for Sand

Cement quantity was held constant at 1306 lbs/yd³ throughout all mixes. Additionally, the admixture Advacast 575 high range water reducer was again used at a ratio of 1.35% to cement for all mixes. All mixes use the same, low w/c ratio of 0.22. Cement, silica powder, and silica

fume carried the highest costs per cubic meter. In order to lower this cost, 2 additional types of cement were identified for their reduced cost, Portland Type V and a Ground Granulated Blast Furnace Slag (GGBS) / Portland I cement blend. Table 3-3 lists the properties for the three cements used in this study. The Type I / GGBS cement blend was identified as a candidate for its exceptional long-term performance (Cheng et al., 2005).

Name	White Cement Type I	Silica Fume	Silica Powder	Cost (\$/yd ³)	Cost Index*
W-25-25	1.00	0.25	0.25	513	1.0
W-30-20	1.00	0.30	0.20	502	0.98
W-35-15	1.00	0.35	0.15	492	0.96
W-25-20	1.00	0.25	0.20	487	0.95
W-25-15	1.00	0.25	0.15	461	0.90
W-25-00	1.00	0.25	0.00	369	0.72
Portland Type V					
PV-25-15	1.00	0.25	0.15	364	0.71
PV-25-10	1.00	0.25	0.10	338	0.66
PV-25-05	1.00	0.25	0.05	307	0.60
PV-30-05	1.00	0.30	0.05	338	0.66
PV-35-05	1.00	0.35	0.05	348	0.68
PV-25-00	1.00	0.25	0.00	282	0.55
PV-25-25	1.00	0.25	0.25	420	0.82
Portland Type I / GGBS Cement					
GG-25-00	1.00	0.25	0.00	266	0.52
GG-25-15	1.00	0.25	0.15	353	0.69
GG-25-25	1.00	0.25	0.25	405	0.79

*Matrix only, without fibers.

Table 3-2: Mixture Proportions by Weight with Cost Index

Type	C ₂ S %	C ₃ S %	C ₂ S + C ₃ S %	C ₃ A %	C ₄ AF %	Blaine m ² /kg
White Cement Portland Type I	13	74	87	5	1	395
Portland Type V Cement	17	59	76	4	15	430
Type I / Slag Cement Blend	13	58	71	8	10	600

Table 3-3: Cement Properties

The cost for silica powder and silica fume was reduced through reductions in material quantities. Ratios for SF ranged from 0.25 SF: C to 0.35 SF: C. Ratios for SP ranged from 0.00 SP: C to 0.25 SP: C. Reduction in the amount of SP was of particular interest due to its high material cost. In some mix designs, when SP was reduced, the amounts of SF were increased since SF and SP have similar particle sizes along their particle size distribution.

3.2.2. Steel Fibers

Steel fiber reinforced concretes resist post-cracking tensile stress through the composite action between the concrete and fibers, including chemical and mechanical bonding at the interface between the two. In this study, all UHPC mixes contain 1.5% steel fibers by volume of the wet concrete. The steel fibers (Figure 3-2) used are brass coated, smooth fibers. Each fiber is 0.75 in (19 mm) long with a diameter of 0.0078 in (0.2 mm) and has a minimum tensile strength of 285 ksi (1965 MPa).



Figure 3-2: Example of the Steel Fibers Used in this Study

3.2.3. Mixing Procedure

Mixing was done using a large Hobart food-type mixer with a 2.65 gal. (10 liter) capacity (Figure 3-3). First, silica fume and the two silica sands were added into the mixer and were dry mixed for approximately 5 minutes at 136 rpm. Silica powder (if any) and cement were then added into the pan and mixed for an additional 5 minutes at 136 rpm. After this, water and the high range water reducer was gradually dispensed into the pan while the mixer was spinning. The blend was allowed to mix for approximately 1-2 more minutes at 136 rpm. Then the mixing speed was increased to 281 rpm for approximately 5 min, or until the concrete reached an acceptable consistency. Once an adequate mixture consistency was achieved, the high strength steel fibers were added into the mixer and allowed to mix at 136 rpm until the fibers were sufficiently dispersed.

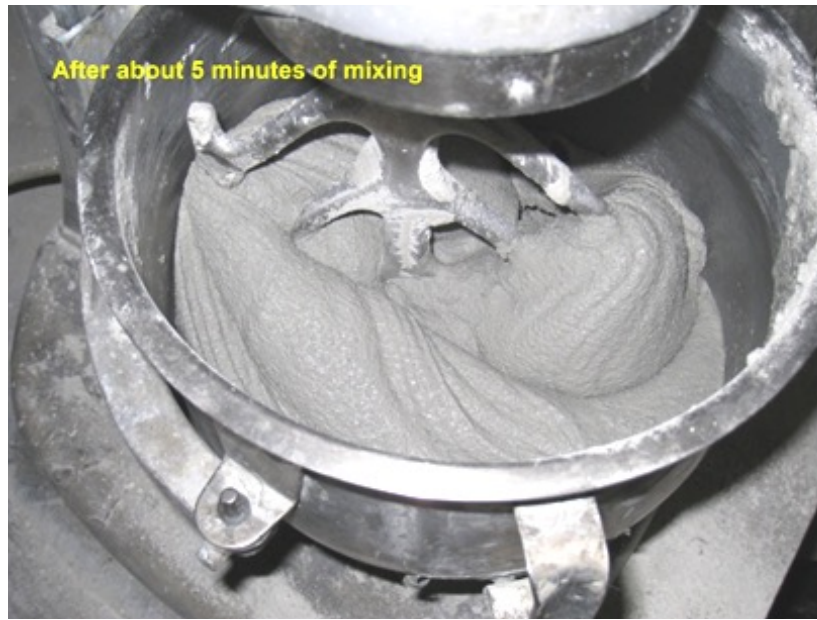


Figure 3-3 Mixing process (photos courtesy of Prof. Kay Wille)

3.2.4. Tensile Strength Testing:

For the purpose of this study, a direct tension test based on AASHTO T 132-87 (2009) was chosen to test the specimens. In this test procedure, precast specimens were made and then tested

under direct tension. As shown in Figure 3-4, the specimens are supported by plates ensuring anchored and rotation-capable boundary conditions.

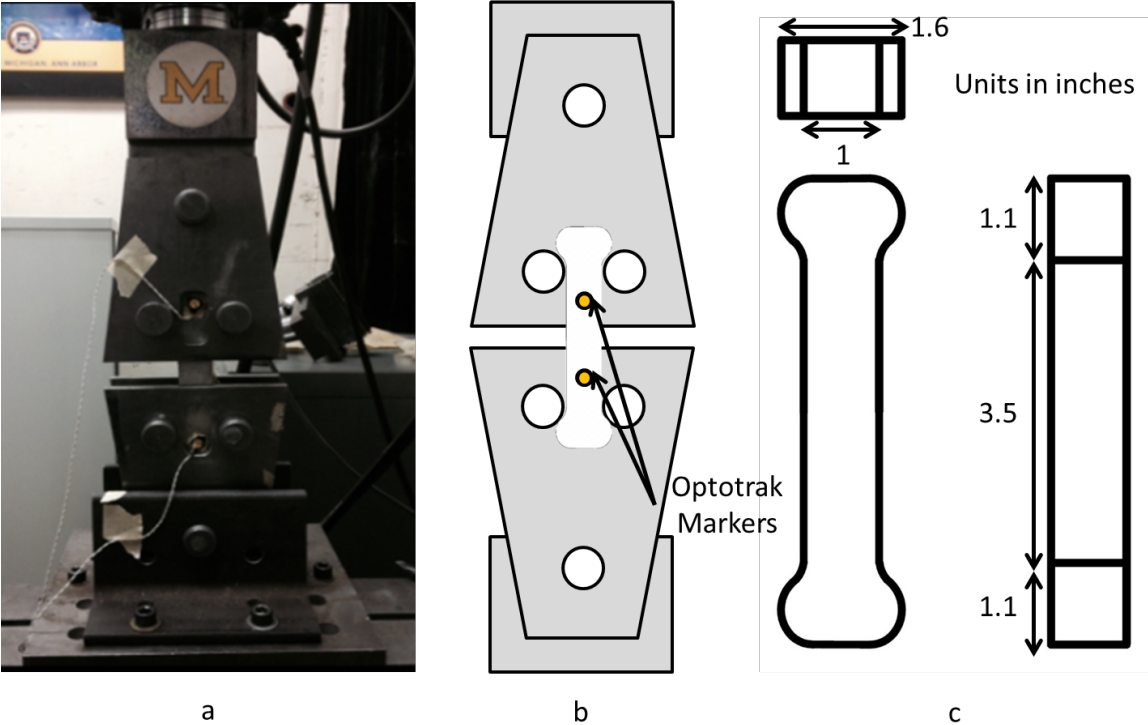


Figure 3-4 (a) Tensile test set up, (b) Instrumentation, (c) Specimen dimensions

Each specimen has a constant cross sectional area of 1 in² (25 mm²) and a gauge length of 3.14 in (80 mm). The long gauge length used enables careful observation for multiple crack development. The UHPC specimens were first mixed in accordance with the procedure prescribed above. They were then poured in layers into dog-bone shaped molds to full capacity. No vibration was used. After initial casting, the specimens were covered and stored at room temperature for 24 hours. Following this, the specimens were removed from the molds and stored in a water tank at 68° F (20° C) for 28 days. Specimens were then given time to dry

(approximately 12 hours) and then tested. For each of the mixes, at least 6 dog-bone tensile specimens were tested and the stress and strain data recorded. Figure 3-5a shows a tested specimen.

Each tensile specimen was carefully loaded into the MTS testing machine. A small preload (20% of the matrix cracking strength) was applied to the specimen, which was then manually moved into the best-aligned position to insure uniaxial tension stress. The loading rate was set to 0.003 in/min those results in an estimated strain rate of $\dot{\epsilon} = 0.0001 \text{ s}^{-1}$. Following the tensile tests, the specimen crack distribution was observed and quantified. Isopropyl alcohol 99.9% was sprayed onto the specimens followed by a blue dye. The contrast in color between the dye and specimen enables a clear visualization of the crack formations.

3.2.5. Compression Testing:

The UHPC specimens were first mixed in accordance with the ratios prescribed above. Compression specimens were poured at once into 2 in. (50 mm) cubed molds. At least 6 compression specimens were tested for each mix and their post cracking strength recorded. The cube specimens were placed into the center of the testing machine and tested in accordance to ASTM C109 (2009). Some specimens were initially precision ground in order to provide a flat surface for testing, however this was later stopped, as it did not yield noticeable differences in strengths between ground and non-ground specimens. Figure 3-5b shows a tested specimen.

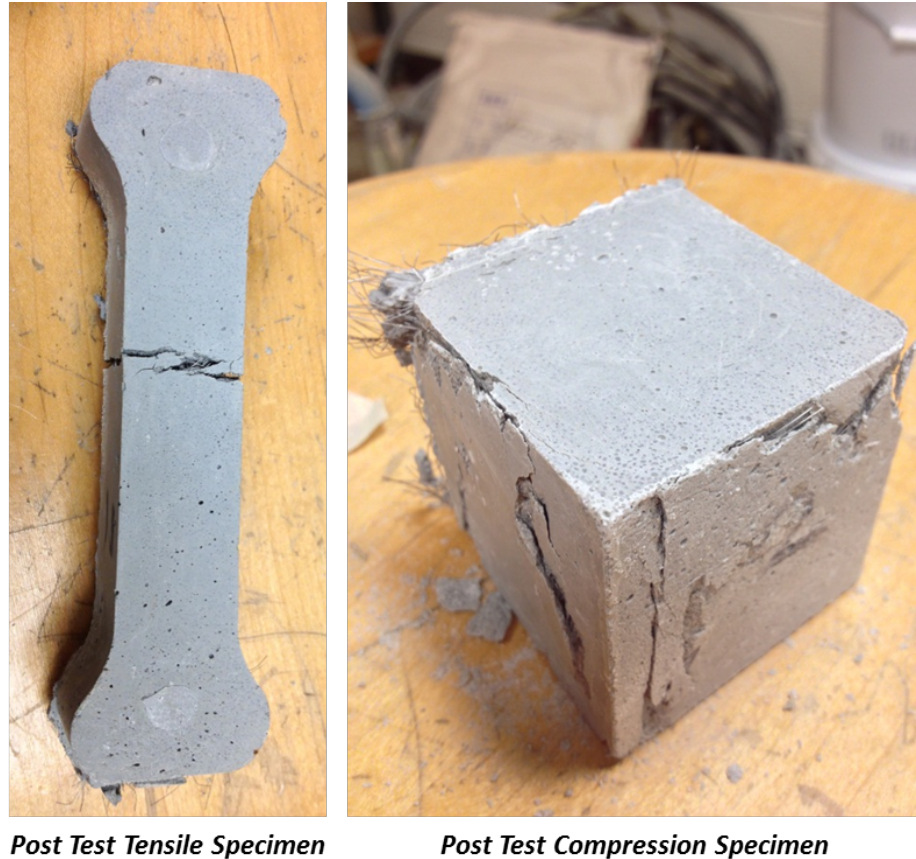


Figure 3-5: Tensile and Compression Specimens Post Test

3.3. RESULTS AND DISCUSSION

3.3.1. Analysis of Data

The following naming scheme was used in order to simplify the discussion of the results. The first number corresponds to the cement type used in the mix design as discussed earlier, W for White Cement Type I, PV for the Portland V and GG for the Portland I / GGBS mix. The second letter refers to the quantity of silica fume present in the mix. The third number corresponds to the quantity of silica powder, and the fourth number corresponds to the steel fiber volume fraction of the UHPC mix design. For example, W-25-25-1.5 would indicate white cement, with 25% silica fume and 25% silica powder, containing 1.5% steel fibers by volume.

For compression, only the maximum compressive strength was considered. For the tensile testing, the test curve was broken down into the three distinct regions as discussed earlier. Adopting the characterization scheme from Naaman (1996), the following parameters were determined: first cracking strength, σ_{cc} , post cracking strength, σ_{pc} , strain capacity, ε_{pc} , energy absorption capacity, g , elastic modulus, E_{cc} , and stress in the fibers, σ_{fpc} . Also, the average number of cracks in the gauge length of the specimen was found. The energy absorption capacity, g , represents the energy absorption capacity prior to tension softening. This graphically corresponds to the total area under the curve up until 95% of σ_{pc} . Experience and experimental data showed that consistent softening behavior occurred in samples beyond this point. E_{cc} represents the elastic modulus of the material and is determined by the slope of the tensile curve prior to initial cracking. The value of σ_{fpc} represents the average fiber tensile stress as determined using the equation proposed by Naaman (1996) and is simply the total post cracking strength divided by 90% of the fiber volume content. This 90% factor is recommended to account for the statistical variability in the experimental procedure. For each set of tensile tests, at least 3 specimen tensile plots are averaged in order to produce a single tensile response curve. The plots are averaged at each point along the strain range. The result is then processed through a moving average filter to account for minute changes due to the sensitivity of the equipment. The average number of cracks is observed visually.

3.3.2. Overview of Results

The tensile and compressive test results produced by the experimental procedure are shown in Table 3-4. The average values between the six specimens tested per experiment were used.

Test Series	Compressive Strength	Post Cracking Strength		Energy Absorption Capacity		Strain Capacity	Fiber Tensile Stress	Average Number of Cracks	Cost Index (\$/\$ Original Mix)*
		σ_{pc}		G		ϵ_{pc}	σ_{fpc}		
	ksi (MPa)	ksi (MPa)		kcal/yd ³ (KJ/m ³)		%	ksi (MPa)	#	
W-25-25-1.5	28.0 (192.7)	1.4 (9.48)		5.5 (30.2)		0.19	101.3 (698)	7.8	1.0
W-30-20-0.5	21.0 (144.7)	0.9 (6.1)		0.6 (3.3)		0.05	196.5 (1354)	1.7	
W-30-20-1.0	23.7 (163.5)	1.2 (8.1)		2.7 (14.9)		0.11	131.2 (904)	5.2	0.98
W-30-20-1.5	28.3 (195.2)	1.4 (9.4)		10.0 (54.7)		0.64	100.9 (695)	8.3	
W-35-15-0.5	20.9 (144.1)	0.8 (5.7)		0.5 (2.6)		0.01	182.7 (1259)	2.2	
W-35-15-1.0	24.0 (165.6)	1.4 (9.7)		3.7 (20.3)		0.16	155.7 (1073)	6.2	0.96
W-35-15-1.5	28.4 (195.4)	1.3 (8.8)		4.3 (23.7)		0.07	94.9 (654)	7.8	
W-25-20-0.5	25.8 (177.6)	0.7 (5.1)		0.7 (4.1)		0.08	164.4 (1133)	2.2	
W-25-20-1.0	27.3 (187.8)	1.0 (7.2)		2.7 (14.9)		0.18	116.5 (803)	4.3	0.95
W-25-20-1.5	28.3 (195.3)	1.6 (10.9)		3.2 (17.5)		0.10	117.3 (808)	7.7	
W-25-15-0.5	26.3 (181.0)	1.1 (7.7)		1.4 (7.6)		0.07	246.9 (1701)	2.3	
W-25-15-1.0	25.8 (177.8)	1.4 (9.6)		5.6 (30.5)		0.10	154.7 (1066)	5.2	0.90
W-25-15-1.5	28.0 (192.7)	1.3 (9.2)		5.3 (29.2)		0.16	99.0 (682)	7.5	
W-25-00-1.5	25.2 (173.8)	1.2 (8.2)		4.0 (21.7)		0.18	88.2 (608)	11.0	0.72
PV-25-15-0.5	20.9 (143.7)	0.9 (6.1)		1.7 (9.4)		0.06	197.7 (1362)	2.5	
PV-25-15-1.0	25.0 (172.1)	1.4 (9.5)		3.2 (17.3)		0.13	152.5 (1051)	6.4	0.71
PV-25-15-1.5	26.6 (183.1)	1.6 (10.7)		6.5 (35.6)		0.11	115.4 (795)	8.3	
PV-25-10-1.5	25.3 (174.4)	1.2 (8.5)		10.5 (57.2)		0.33	91.6 (631)	10.5	0.66
PV-25-05-1.5	26.4 (182.0)	1.2 (8.1)		7.6 (41.6)		0.50	86.5 (596)	10.7	0.60
PV-30-05-1.5	25.0 (172.4)	1.2 (8.2)		7.0 (38.5)		0.27	87.8 (605)	11.0	0.66
PV-35-05-1.5	25.7 (177.2)	1.0 (7.2)		3.7 (20.2)		0.24	77.5 (534)	10.5	0.68
PV-25-00-0.5	22.2 (152.9)	0.6 (4.1)		1.4 (7.4)		0.15	132.8 (915)	2.4	
PV-25-00-1.0	23.5 (161.7)	1.1 (7.6)		6.4 (35.1)		0.11	122.9 (847)	5.6	0.55
PV-25-00-1.5	25.3 (174.0)	1.3 (9.0)		6.4 (35.1)		0.11	96.7 (666)	8.1	
PV-25-25-1.5	27.6 (190.0)	1.3 (8.8)		3.4 (18.7)		0.15	94.5 (651)	10.0	0.82
GG-25-00-1.5	25.2 (173.8)	1.2 (8.0)		3.2 (17.6)		0.15	86.4 (595)	9.0	0.52
GG-25-15-1.5	26.2 (180.6)	1.2 (8.6)		4.4 (24.2)		0.21	91.9 (633)	10.5	0.69
GG-25-25-1.5	26.9 (185.5)	1.4 (9.4)		7.4 (40.5)		0.28	101.5 (699)	11.3	0.79

*Matrix only, no fibers.

Table 3-4: Cost and Performance Summary

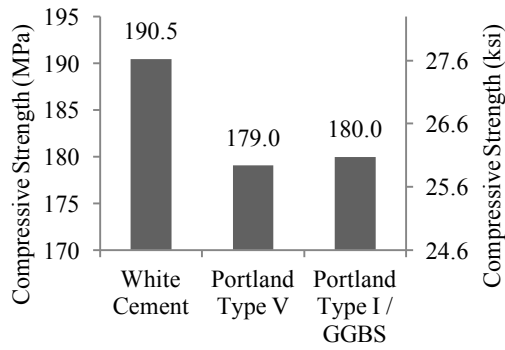
3.3.3. Cement Type

Three different cements were tested with three different mix ratios. Figure 3-6 shows the effects of cement types on various performance parameters for mixes with 1.5% volume fiber fraction. From Figure 3-6a, it can be seen that the compressive strength of the material varies slightly with differences in cement type. In general, the mixes containing the Portland Type V mixes perform the worst, averaging 25.9 ksi (179 MPa). Slightly better, those containing the GGBS / Portland Type I cement achieved on average 26.1 ksi (180 MPa) in compression. Those containing the White cement performed the best, averaging 27.7 ksi (191 MPa). All three cements performed above the minimum required compressive strength to qualify as UHPC, i.e. 22 ksi (150 MPa).

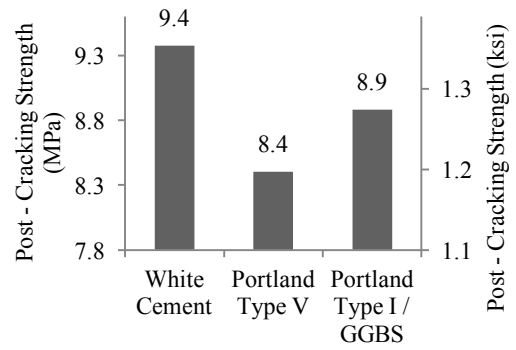
In tension, the average post cracking strength for each mix was also considered. From Figure 3-6b, White Cement mixes exhibited the highest tensile strength, averaging a max post cracking strength of 1.3 ksi (9.3 MPa). Portland Type V mixes averaged the lowest strengths, 1.2 ksi (8.4 MPa) and those containing GGBS / Portland Type I mixes achieved average post crack strengths of 1.3 ksi (8.9 MPa). All specimens showed at least 8 cracks in the gage length (Figure 3-6c), while specimens containing the GGBS / Portland Type I cement exhibited the most cracking. All specimens exhibited strain hardening and had a strain capacity, ε_{pc} , ranging from 0.21 to 0.24 (Figure 3-5d). Similarly, the energy absorption capacity (Figure 3-6e) and fiber tensile stress (Figure 3-6f) for all three cement types showed little variation and no clear trend between the three cement types. While specimens containing white cement performed the best in compression, all three cements showed good performance under tension and compression indicating they are all suitable for UHPC.

3.3.4 - Silica Powder

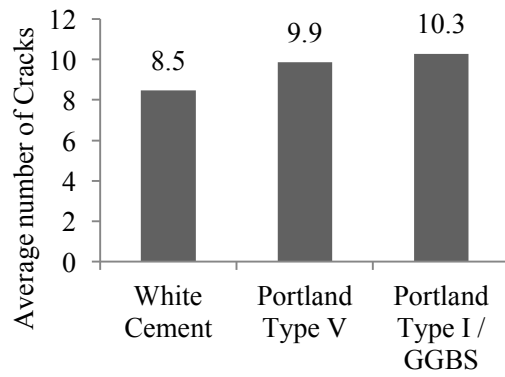
Figure 3-7 shows the effects of SP on various performance parameters for all mixes with 1.5% volume fiber fraction. From Figure 3-7a, it's seen that compressive strengths ranged from 25.1 ksi (173 MPa) at 0% SP up to 27.1 ksi (187 MPa) at 25% SP. Compressive strengths increased as SP increased up to 20%, dropping slightly as SP increased further to 25%. In tension, post cracking strengths (Figure 4b) showed little variation, with specimens containing 0% SP achieving 1.2 ksi (8 MPa) up to 1.4 ksi (9.5 MPa) for those containing 25% SP. Similarly, the average number of cracks formed showed little change from 0% SP to 25% SP. Energy absorption capacity decreased slightly from 0% SP to 20% SP, though 25% SP showed the greatest energy absorption capacity. Fiber tensile stresses essentially remained unchanged, indicating SP did not affect the ability of the fibers to transfer load. Figure 3-7 shows that significant changes in SP content resulted in minor changes in all the performance parameters.



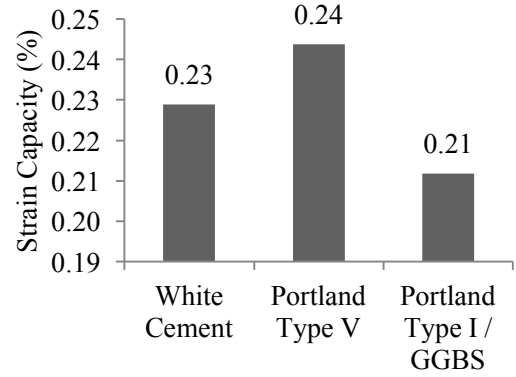
a



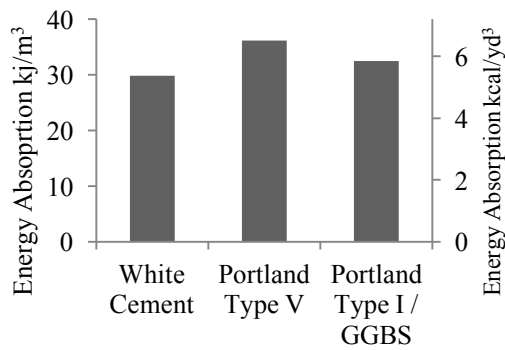
b



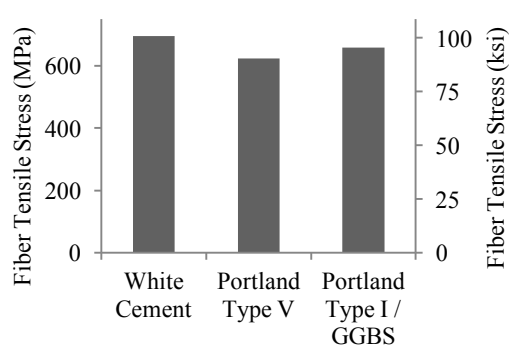
c



d

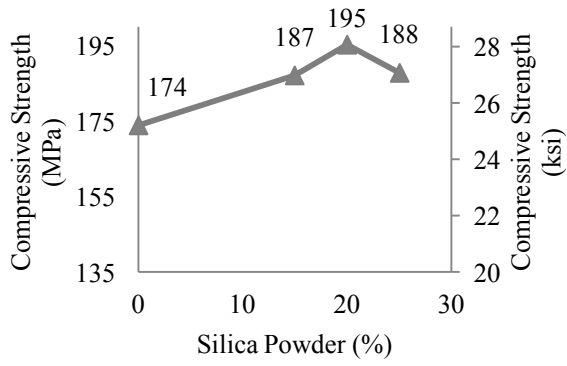


e

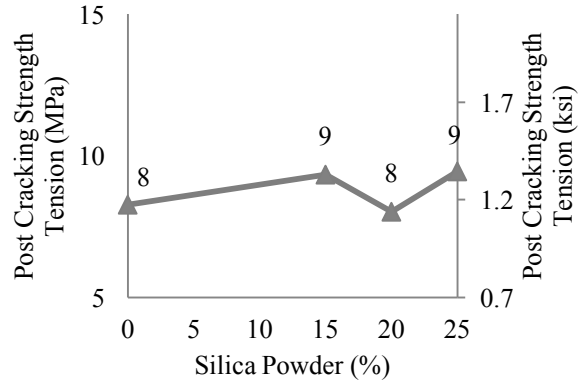


f

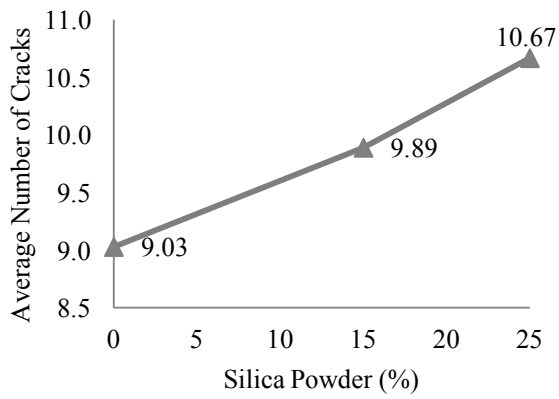
Figure 3-6: Effects of Different Cements on UHPC for Mixes with 1.5% Volume Fiber Content



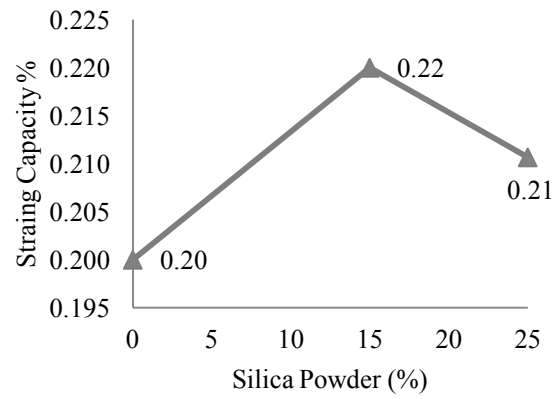
a



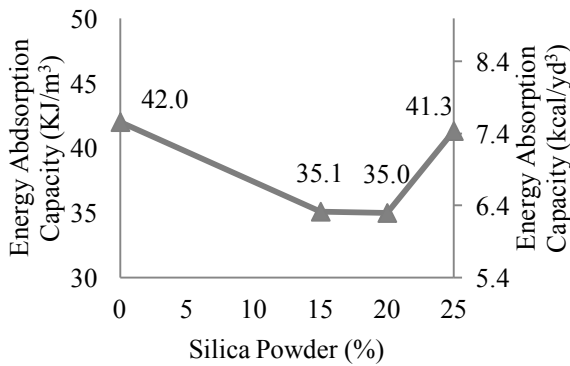
b



c



d



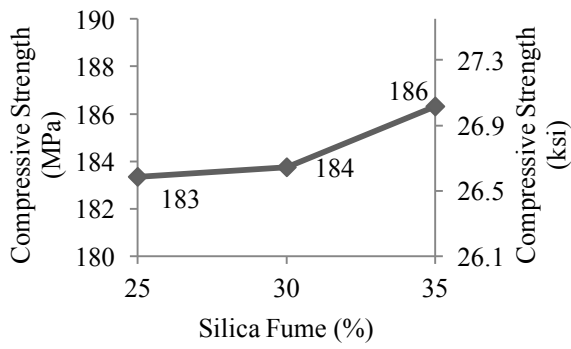
e

Figure 3-7: Effects of Silica Powder Content on UHPC for Mixes with 1.5% Volume Fiber Content

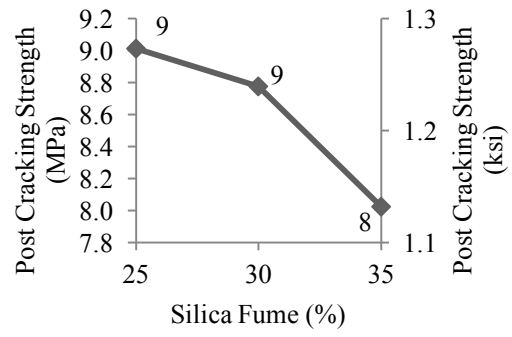
3.3.4. Silica Fume

Three different ratios of silica fume were tested. Figure 3-8 shows the effects of silica fume on various performance parameters for all mixes with 1.5% volume fiber fraction. In Figure 3-8a, the compressive strength of the material varies slightly with variation in silica fume. Mixes containing 25% SF averaged 26.7 ksi (184 MPa), increasing up to 27 ksi (186 MPa) for those containing 35% SF. This accounts for less than a 1.5% variation in compressive strength at increases in SF up to 15%.

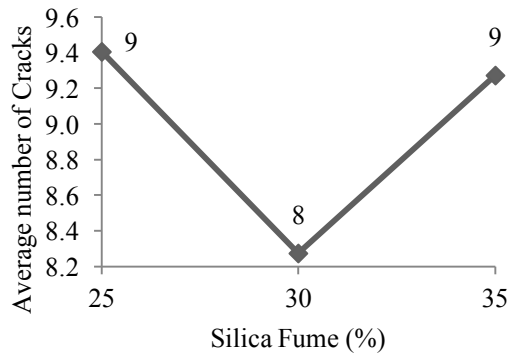
Similarly, in tension, the results showed slight changes with variations in silica fume. Post cracking strengths (Figure 3-8b) for mixes containing 25% SF averaged 1.3 ksi (9 MPa) decreasing with additional SF; 35% SF averaged 1.2 ksi (8 MPa) in tension. This accounted for an 11% difference in strengths for a 15% increase in SF. The average number of cracks for all mixes was above 8 (Figure 3-8c), again indicating good strain hardening behavior. Strain capacity for all SF percentages ranged from 0.2% to 0.24%. Energy absorption (Figure 3-8e) decreased somewhat as SF content increased. While the changes in compressive strength were minimal, increased SF content led to lower performance under tension, and a reduction in fiber tensile stress indicated a decrease in the ability of the steel fibers to carry tensile forces.



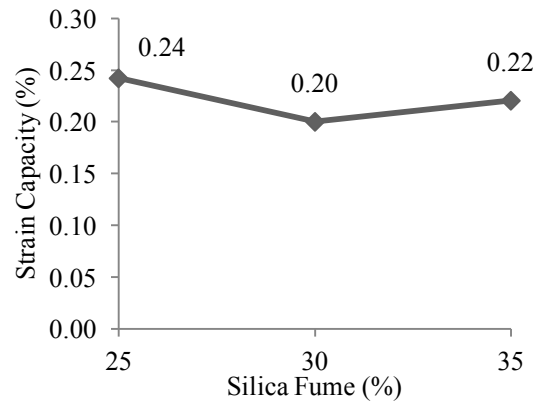
a



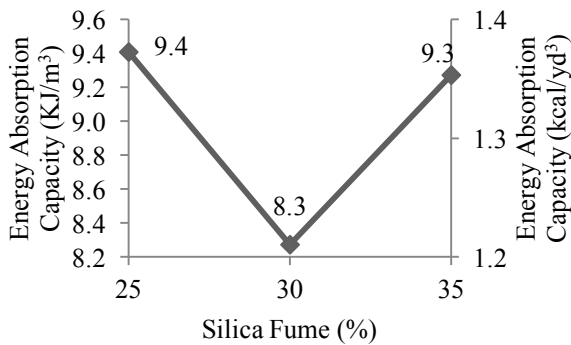
b



c



d



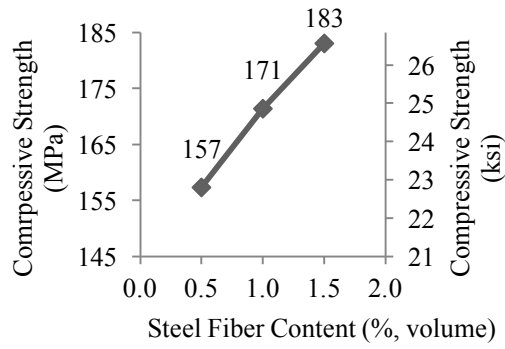
e

Figure 3-8: Effect of Silica Fume Contents on UHPC for Mixes with 1.5% Volume Fiber Content

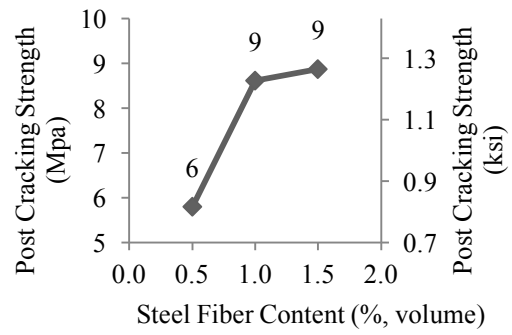
3.3.5. Fiber Content

Figure 3-9 shows the effect of fiber volume fractions averaged across all performance parameters for the various mixes. As seen in Figure 3-9a, compressive strength ranges from 22.7 ksi (157 MPa) at 0.5% fibers by volume to 26.5 ksi (183 MPa) at 1.5% fibers by volume, a difference of 15% in strength capacity. Compressive strength of the specimens increased linearly with increases in fiber content. In tension, specimens containing 1.5% fibers yielded the highest average post cracking strength (Figure 3-9b) averaging 1.3 ksi (9.0 MPa), while those containing 0.5% fibers were the lowest at 0.8 ksi (5.8 MPa). Similarly, the strength increases linearly with respect to increasing fiber content. The remaining tensile properties also increased almost linearly with an increase in the steel fiber content (Figure 3-9c, d, e). The fiber tensile stress decreased with increasing fiber content, as more fibers were available to transfer the load. The decreased stress in the steel fibers is also likely affected by the fiber-group effect, which reduces the matrix's ability to resist the bond. These results are in line with what has been observed in other fiber reinforced concretes (Wille et al, 2012).

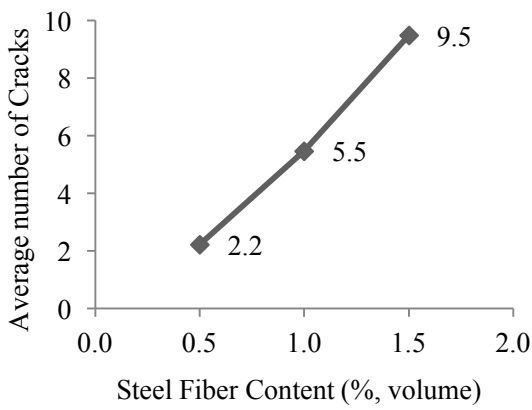
Figure 3-10 shows the average tensile stress-strain response for specimens containing 0.5%, 1.0% and 1.5% steel fibers by volume, while Figure 3-11 shows the data in another format for clarity. The average tensile response curve was calculated taking the mean value of the stress for each strain value for each of the tests performed in the series. It is clear that strain hardening is achieved for all fiber contents studied in this work. At 0.5% steel fibers, the strain capacity is 0.07%. This almost doubles to 0.13% as the fiber volume fraction increases to 1%. At 1.5% volume fraction, the strain capacity is 0.23.



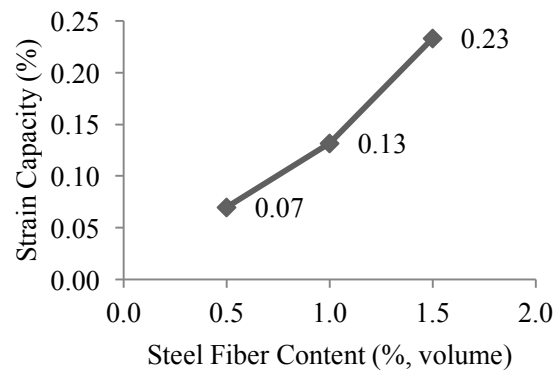
a



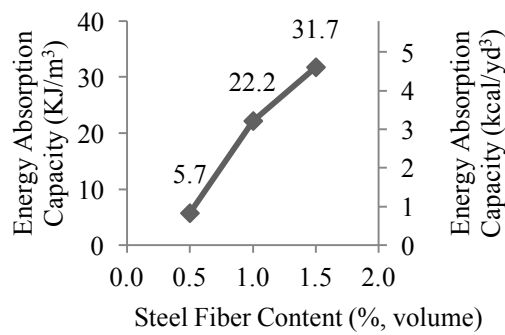
b



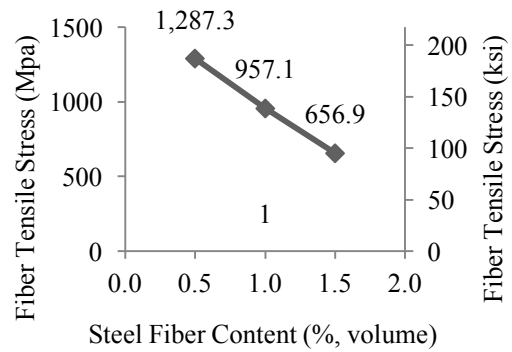
c



d



e



f

Figure 3-9: Effects of Lower Steel Fiber Volume Contents on UHPC

In most structural applications, construction grade reinforcing steel yields at 0.2% strain. Assuming that the live and dead loads on a structure are equal, load factors for them to be 1.4 and 1.7 according to ASCE7 (2010) respectively, and the only forces on a structure, the strain in steel bars can be estimated to be 0.09% under dead loads alone and 0.13% under working conditions. Using a tensile strain hardening material that has a strain capacity that is at least one of these values will limit crack localization and protect the steel from moisture and ingress of chlorides.

It appears from the test results provided that using UHPC with 0.5% volume fiber content could come close to the lower bound (0.09%). However, the tensile coupons conducted in this work tend to align fibers preferentially along the load direction. In a real structure, the fibers will be randomly oriented, resulting in a lower effective volume fraction in any particular direction. Hence it is unlikely that UHPC with 0.5% volume fraction can provide sufficient strain hardening to eliminate crack localization under dead loads. However, UHPC with 1% fibers likely is able to do so, and with 1.5% fibers, the protection likely extends beyond just dead loading and into working conditions. Clearly, the observations pertaining to structural behavior must be evaluated through full-scale structural tests.

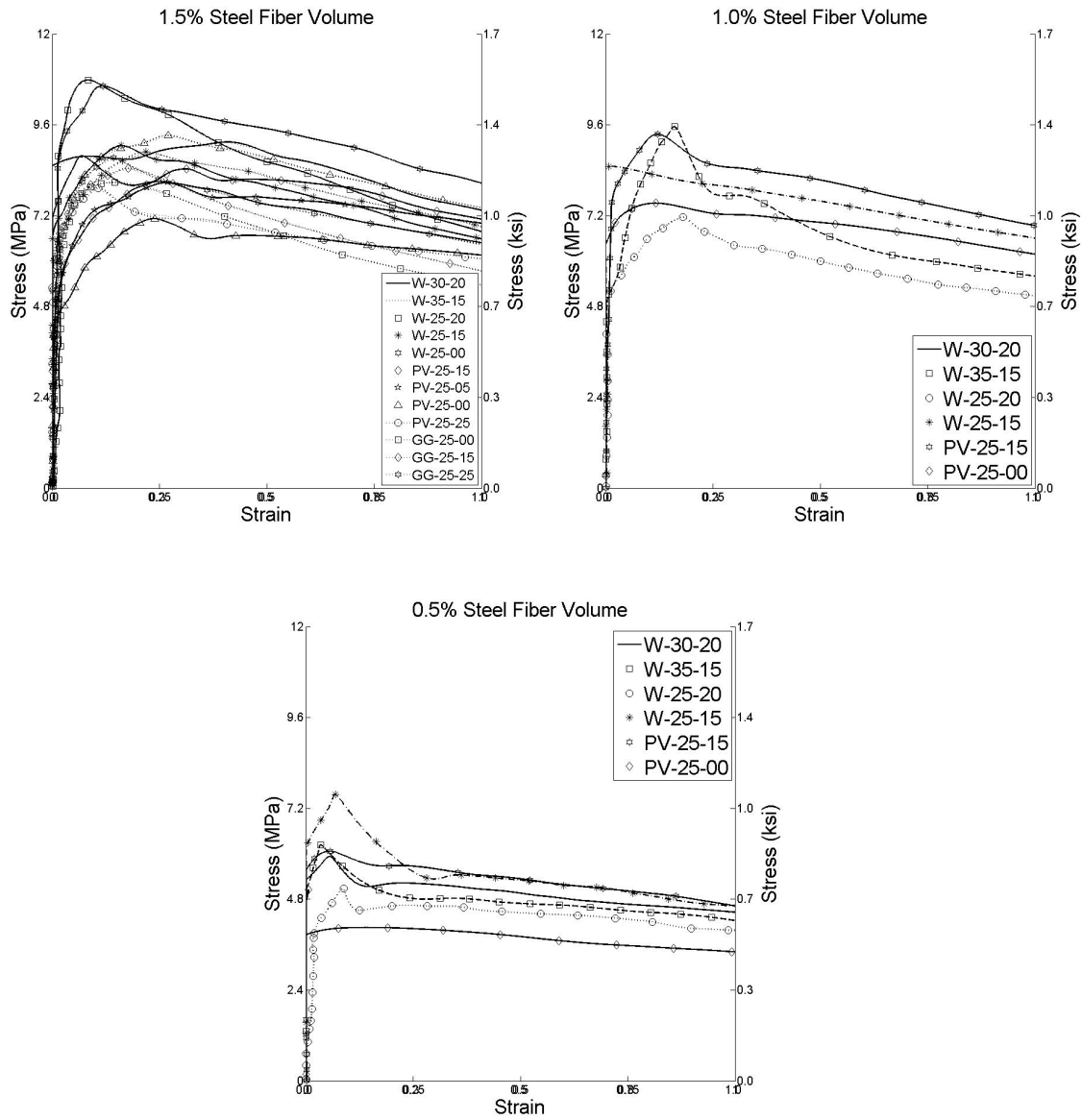


Figure 3-10: Strain Response for UHPC Specimens in Tension

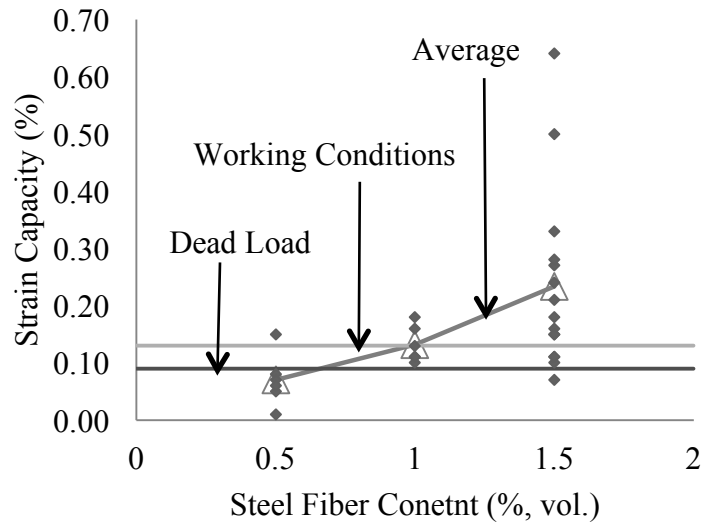


Figure 3-11: Strain (%) Capacity as function of Steel Fiber Content

3.3.6. Cost Analysis

The cost indices for each of the UHPC mixes tested are listed in Table 3-4. All of the costs used to calculate the cost index are for the cementitious materials alone, excluding the cost of steel fibers. Steel fibers, produced and sold in the US, would add an additional cost of approximately \$516/yd³ for every 1% increase in fiber content by volume, or increase the cost index by 1.0. Figure 3-12 shows the compressive strengths for all the specimens tested vs. cost index. As can be seen, compressive strength increases linearly with increased cost. In general, cost was the highest in specimens containing the white cement, and lowest in those containing the Portland Type I / GGBS mix, as is consistent with their material costs. The least expensive mix, GG-25-00, contained 0% silica powder and used the Portland Type I / GGBS blend. Its cost index of 0.52 represents a 48% reduction in cost compared to the starting mix (5), W-25-25. Considering its lowered cost, and overall good performance, GG-25-00 presents the most optimal performance vs. cost mix of those tested. Details of this mix can be found in Table 3-5.

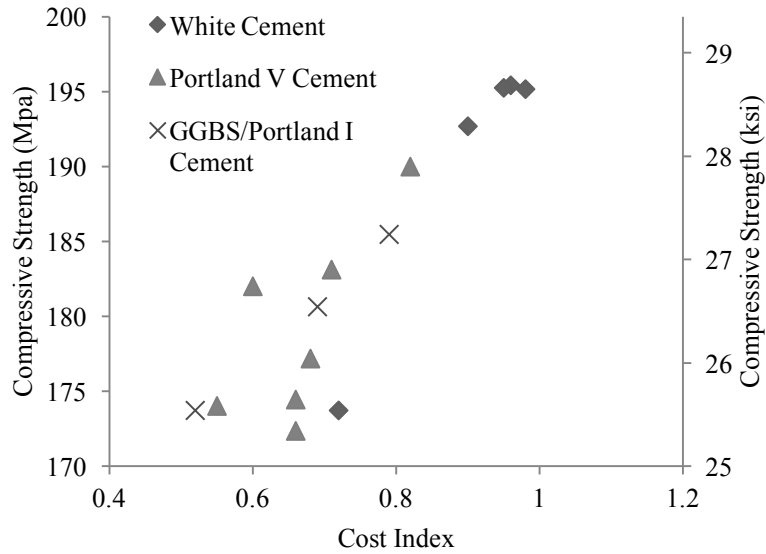


Figure 3-12: Compressive Strength as a function of Cost Index

Type	UHPC Ratio	kg/m ³
Cement	1	775
Silica Fume	0.25	194
Water	0.22	165
High Range Water	0.0054	10
Fine Sand I	0.26	245
Fine Sand II	1.03	975

Table 3-5: UHPC Mix Design and Ratios

3.4. CONCLUSION

The objective of this study was to optimize a UHPC mixture through modification of the material's constituents. Several parameters were considered, and designs were created and tested. Each design was assigned a cost index value, and ultimately a recommendation was made. The conclusions of this study are as follow:

- All of the mixes tested achieved sufficient strengths in compression for them to be labeled as UHPC.
- All three cements tested performed comparably well in tension and compression. White cement yielded the high compressive strengths, but the Portland Type I / GGBS Cement blend carried the lowest cost, thus making it a good, cost-effective choice for future UHPC mixes.
- Changes in silica powder content yielded little variation in the performance parameters examined. In particular, specimens containing no silica powder were all within 5% of the strength in tension and compression. Due to its high cost and minimal beneficial effects, silica powder could be eliminated from UHPC mixes to reduce cost.
- Changes in silica fume led to minimal changes in compressive strength. Increased SF content led to somewhat lower performance under tension, and a reduction in fiber tensile stress indicating a slight decrease in the ability of the steel fibers to carry tensile forces.
- The results suggest that fiber volume contents of 1.0% or 1.5% could significantly reduce the chance for crack localization under dead load or working conditions, respectively, in structural applications.
- Mix GG-25-00 had the lowest cost index, while still maintaining ultra-high performance, making it the recommended mix from this study. Additionally, the availability of GGBS and Portland Type I cement make it an appealing choice for use in further UHPCs.

Intentionally left blank